

Morphological Characteristics of OB Spectra and Environments

Nolan R. Walborn¹

¹ Space Telescope Science Institute, Baltimore, Maryland, USA

Abstract

Following a brief exposition of the morphological process, two examples of its application in contemporary astronomy are presented. The first comprises a major digital, blue-violet spectral classification program on Galactic O stars, that has already revealed three special categories or new members thereof: the Ofc class with C III $\lambda 4650$ emission comparable to N III $\lambda 4640$, the Of?p class of magnetic oblique rotators, and the ONn class of nitrogen-rich rapid rotators. All of these categories portend further understanding of massive stellar atmospheres and evolution. The second example concerns the structure of massive young clusters and nebulae as a function of age on timescales of the order of or less than 10 Myr, which has provided a new insight into the Antennae major-merger starburst.

1 The Morphological Process

The morphological method in astronomy comprises the description of unknown objects, in terms of certain well-defined criteria, differentially with respect to a reference frame of standard objects selected from the data themselves. This approach will organize the empirical characteristics and often discover new ones, distinguish the normal majority from peculiar exceptions, and suggest or eliminate interpretational hypotheses. An essential element of the process is rigorous independence from external information, which ensures permanent validity of the description, independently of errors in or revisions to the subsequent calibration and interpretation. Of course, morphology does not explain anything; rather, it properly formulates the phenomena to be explained.

These concepts are displayed and interrelated graphically in the Walborn Diagram (Figure 1) both in general astronomical terms and in those specific to spectral classification and stellar astrophysics. The key point is the existence of an intermediate category, our Image of Nature, between Nature itself and the ultimate objective of understanding Nature. The role of morphology is to establish an Image that is sufficiently accurate, complete, and

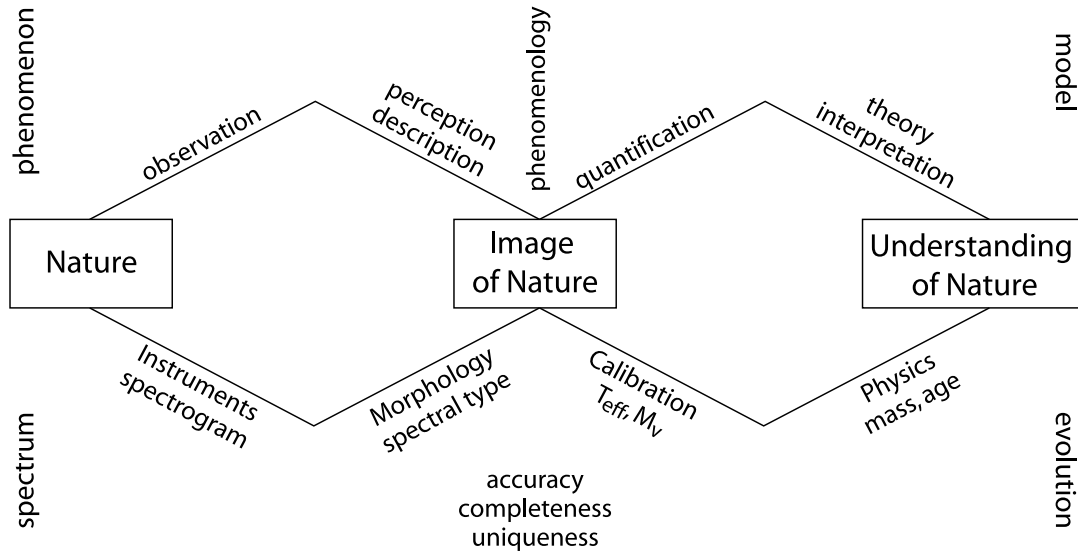


Figure 1: The Walborn Diagram, which displays the operations linking Nature, our Image of Nature, and our understanding of Nature, in both general terms above and those specific to spectral classification or stellar astrophysics below.

unique to be usefully calibrated and interpreted. Common errors are failure to recognize the existence or significance of the intermediate category, confusion among the categories, and convolution of operations that should be sequential instead. When the Image is inadequate, no amount of physics will provide correct understanding.

2 OB Spectra

Stellar spectral classification in the violet-blue-green optical wavelengths had its origins during the late 19th century, and it provided the foundation of 20th century astrophysics. Yet as illustrated in the following subsections, this technique continues to reveal new phenomena today. The recent compendium *Stellar Spectral Classification* (Gray & Corbally 2009) provides a definitive reference on the subject. It provides a valuable compilation of history, techniques, classification criteria, and standard stars. In particular, Chapter 3 on the OB stars presents pertinent developments through the first decade of the 21st century, including the remarkable correlations among the optical, ultraviolet, infrared, and even X-ray spectra, which are leading current developments in many areas of astrophysics.

2.1 GOSSS

A major optical spectroscopic program led by J. Maíz Apellániz at the Instituto de Astrofísica de Andalucía, the Galactic O-Star Spectroscopic Survey (GOSSS), is acquiring moderate-

resolution, high-S/N digital observations of all known Galactic O stars and many of type B to about 13th mag, about 2000 objects (Sota et al. 2011). This unprecedented combination of quality, sample size, and homogeneity is improving the systematic and random accuracies of the classification, as shown in a new spectral atlas. An expected corollary is the discovery of new objects and categories of special interest. Three examples are described next.

2.2 Ofc Spectra

Of spectra are defined by their selective emission lines of He II $\lambda 4686$ and N III $\lambda\lambda 4634-4640-4642$; the gradual development of these features is the basis of the O-type luminosity classification. A few otherwise normal Of supergiants with comparable C III $\lambda\lambda 4647-4650-4652$ emission lines had been known, but the GOSSS data show for the first time that this characteristic is frequent near spectral type O5 at all luminosity classes and also increases gradually with luminosity (Walborn et al. 2010; Figure 2 here). It likely represents a new selective emission feature (Walborn 2001), i.e. emission in particular transitions caused by anomalous level population effects, which are very sensitive diagnostics of the atmospheric and wind parameters (e.g., Corti, Walborn, & Evans 2009). Moreover, the C III emission appears to be present in some clusters and associations but not others, possibly hinting at N/C abundance differences among them.

2.3 Of?p Spectra

The Of?p notation was introduced in the early 1970's to emphasize doubt that three very peculiar and similar spectra corresponded to normal Of supergiants. In addition to C III $\lambda\lambda 4647-4650-4652$ emission lines comparable to N III $\lambda\lambda 4634-4640-4642$, they showed evidence of circumstellar activity in terms of sharp absorption features and P Cygni profiles at H and He I lines. During the past decade, all three have been shown to be extreme, periodic spectrum variables, and soon thereafter their strong magnetic fields were detected (Martins et al. 2010, Wade et al. 2011), revealing them as O-type magnetic oblique rotators. GOSSS has already increased the membership of this rare category to five (Walborn et al. 2010; Figure 3 here); references to the prior developments can be found there.

2.4 ONn Spectra

The causes and effects of rotation in massive stellar evolution, involving mixing or transfer of processed material to the surface and enhanced mass loss, are active areas of current research (Maeder & Meynet 2000; Walborn 2003; Langer et al. 2008). In particular, enhanced N/C abundance ratios in the atmospheres and winds are a vital diagnostic of these effects. The most rapidly rotating O star known, HD 191423, was shown to be nitrogen-enriched by Howarth & Smith (2001). GOSSS has already discovered two clones of this spectrum and confirmed several other less extreme but still rapidly rotating, late-O giants as members of this category (Walborn et al. 2011; Figure 3 here). These spectra may well provide significant insights into the evolution of rotation and mixing between the main-sequence and supergiant stages, in the corresponding mass range.

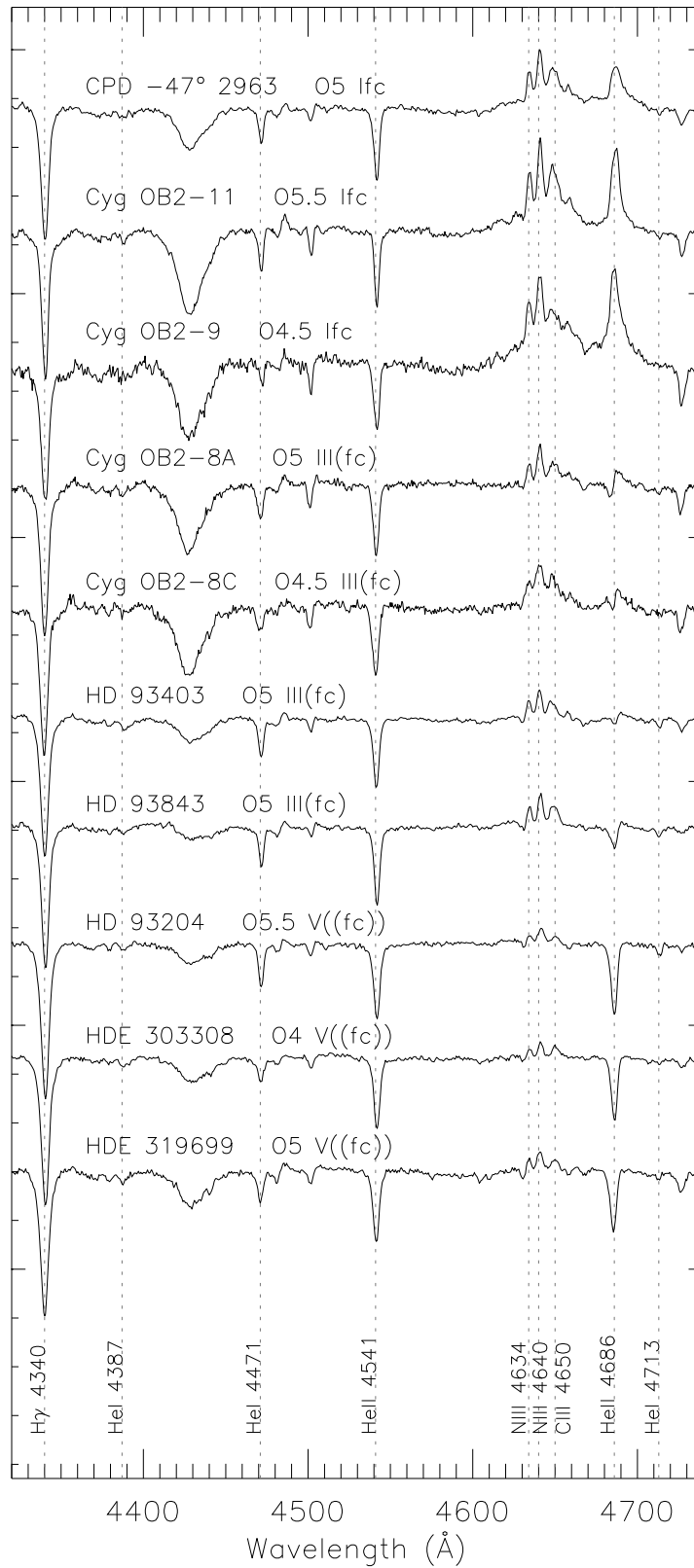


Figure 2: A luminosity sequence of Ofc blue-green spectra. The longer ordinate tick marks are separated by 0.5 rectified continuum intensity units. From Walborn et al. (2010).

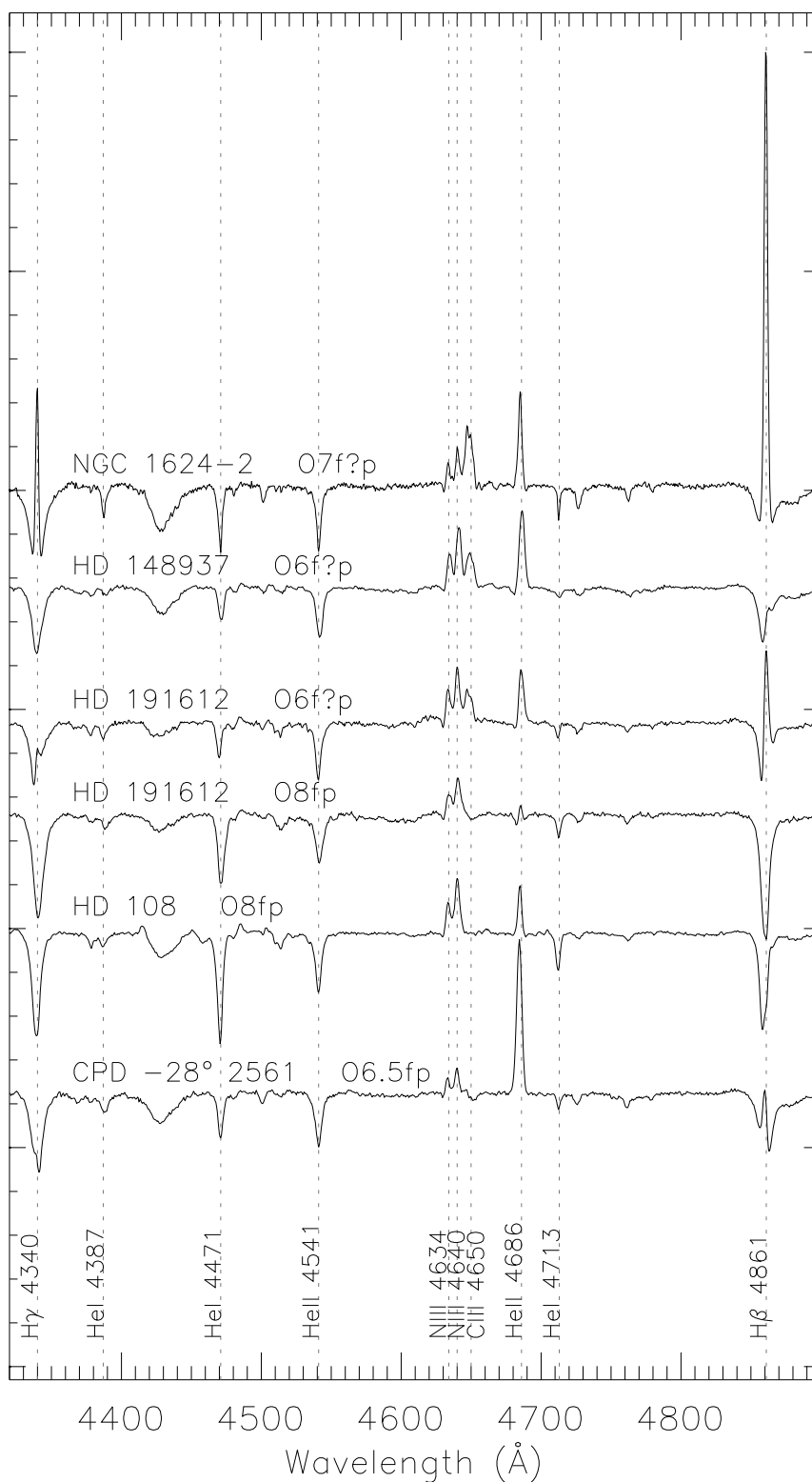


Figure 3: Of?p blue-green spectra. HD 108, 148937, and 191612 are the original members of the category; the last is shown in both maximum and minimum states. NGC 1624-2 was discovered to belong to this class by GOSSS, while the membership of CPD $-28^{\circ}2561$ was first established by the associated high-resolution southern survey led by R. Barbá and R. Gamen (although a low-resolution observation is shown here). From Walborn et al. (2010).

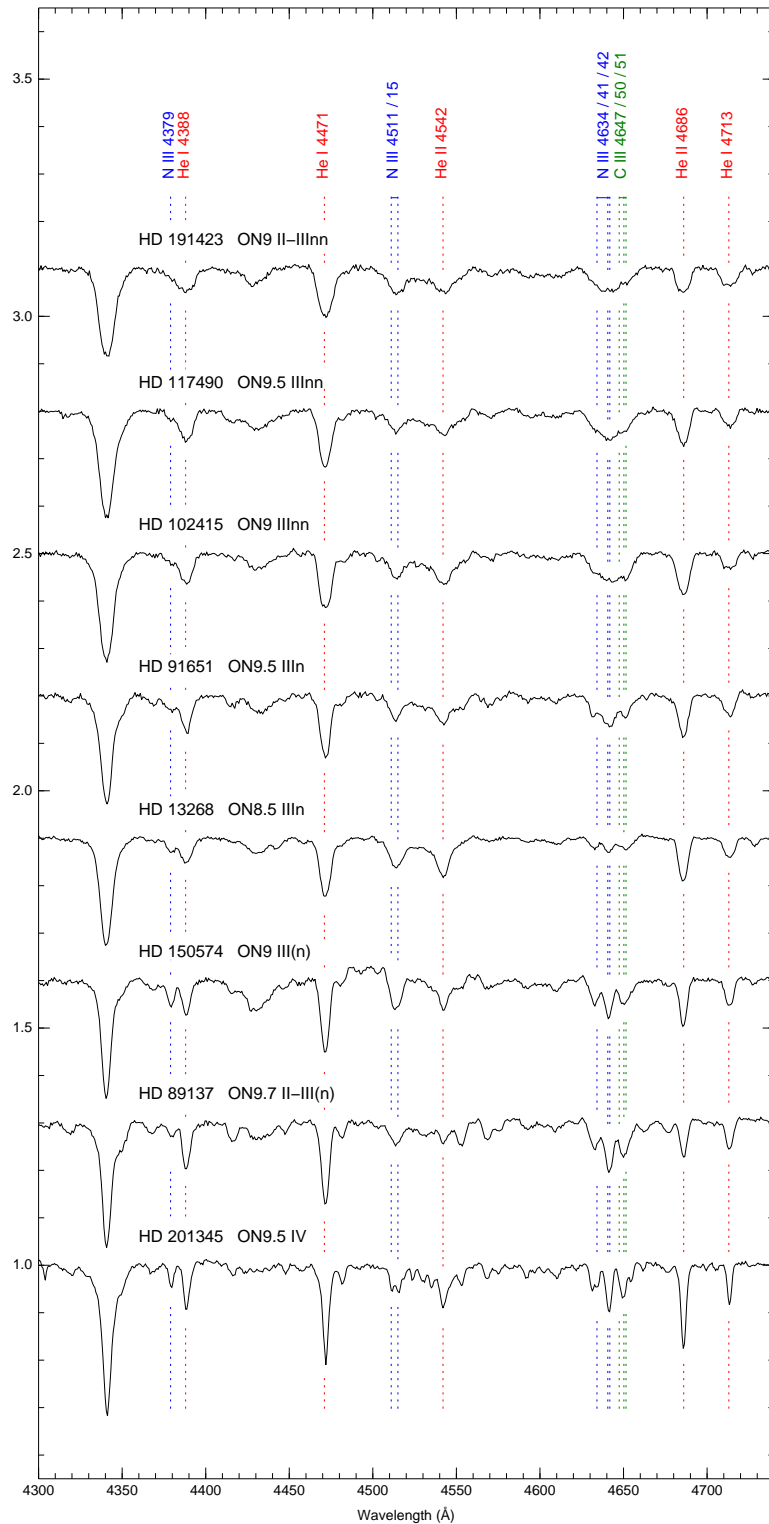


Figure 4: A $v \sin i$ sequence of ONn blue-green spectra. All of these late-O giants (luminosity class III) and bright giants (II) are strongly nitrogen-enhanced (“N”) and rapidly rotating (“n”). The approximate $v \sin i$ ’s corresponding to (n), n, and nn are 200, 300, and 400 km sec^{-1} , respectively. HD 191423 is Howarth’s Star, while HD 102415 and 117490 are newly discovered as members of this category by GOSSS. The more slowly rotating subgiant (IV) HD 201345 is shown for comparison. To be further discussed by Walborn et al. (2011).

3 OB Environments

Because of the short timescale for massive stellar evolution, the structure and content of the spectacular clusters and H II regions in which most young massive stars are found also evolve qualitatively over the first 10 Myr. These evolving characteristics allow quite precise dating of massive young clusters, to large distances in high-resolution images, from their morphology alone, as further discussed below.

3.1 Age Paradigms

Table 1, from Walborn (2010), provides a standard sequence of young clusters in terms of several well-defined parameters. The latter are derived from essentially complete (calibrated) spectral classification of the massive stellar content in these nearby Galactic objects. The degree to which all of these parameters are correlated in coeval systems is remarkable. As a result, objects that are too distant for detailed study of their stellar content can be classified into these evolutionary stages by their global morphologies alone.

Table 1: Characteristics of massive young cluster age paradigms

Object	Visually	MS Turnoff		Age [yrs]	H II, Dust	Red Sg
	Brightest Stars	Spectrum	Mass[M_{\odot}]			
Orion Nebula	ZAMS O, (IR)	(PMS)		$< 10^6$	Yes	No
Carina Nebula	O2, WNL	O3	100	$1-2 \times 10^6$	Yes	No
Scorpius OB1	OB Sg	O6	50	$3-4 \times 10^6$	No	No
Westerlund 1	AF Sg	O7–O8	35	$4-5 \times 10^6$	No	Yes
Perseus OB1	AF Sg	B0–B1	20	$7-9 \times 10^6$	No	Yes

3.2 Two-Stage Starbursts

The next step in understanding massive young regions is the realization that many or most of them consist of two phases from the preceding sequence: an older first generation and a second, triggered generation at the periphery, usually or always concentrated to one side (Walborn 2002). (This latter characteristic possibly indicates that the initial collapse is triggered externally near the surface, rather than globally toward the center of the precursor giant molecular cloud.) Thus, 30 Doradus in the Large Magellanic Cloud contains a Carina-phase first generation and an Orion-phase second generation (Walborn et al. 1999a; Walborn, Maíz Apellániz, & Barbá 2002), while the second-ranked LMC H II region Henize N11 is a giant shell with a Scorpius OB1-phase central association in a completely evacuated cavity and Carina-phase nebulae at the periphery (Walborn & Parker 1992; Walborn et al. 1999b). In both cases the age *difference* between the two generations is ~ 2 Myr, but the absolute ages are greater in N11. In the LMC objects, these conclusions are also based on complete spectral

classification of the massive stellar contents. But then, the global properties of similar regions in more distant galaxies can be used to date them even though detailed spectral classification is not yet possible. E.g., NGC 604 in M33 is very similar to N11. Even entire, recent star-formation subregions in some galaxies can be sequentially dated in this way, e.g. NGC 4214 (Mackenty et al. 2000), NGC 2363 (Drissen et al. 2000), and NGC 6946 (Larsen et al. 2002).

3.3 The Antennae Revealed

The Antennae, at a distance of about 20 Mpc, constitute the nearest major merger and are thus a key system for understanding this phenomenon, which is ubiquitous at greater distances in the earlier Universe. Accordingly, it has been the subject of intensive investigation. With HST imaging, Whitmore et al. (2010) have shown that it contains several hemispheric two-stage starbursts with global structures very similar to those of the nearby objects discussed above, despite their larger dimensions in the Antennae. Three recent papers (Zhang et al. 2010, Karl et al. 2010, Teyssier et al. 2010) have established a timescale of order 10 Myr for the observed starburst, corresponding to the periastron passage in progress; Teyssier et al. even derive the essential result that the starburst is distributed rather than nuclear. The current interaction region of the two spiral disks has been identified with an extreme concentration of dust clouds and luminous infrared sources revealed by Spitzer (Wang et al. 2004) and Herschel (Klaas et al. 2010). Nevertheless, the predominant structure of the global starburst in the Antennae has not yet been clearly recognized. It is readily discerned by the above morphological procedures as a distorted Z-shaped age sequence (“The Mark of Zorro”) across the entire face of the system, avoiding the galactic nuclei, as shown in Figure 5. The annotated ages are based on the structures (or absence) of the nebulae and clusters in the corresponding subregions, ranging from the pure dust/IR sources through, consecutively, centrally concentrated H II regions, giant shells, and dissipating nebulosities, to a region of bright blue stars and possibly red supergiants without any nebulosity. The intensity of the IR emission in the Spitzer images declines along the same sequence, with a single notable exception that may correspond to multiple generations at the site of a giant shell (“S” in the nomenclature of Whitmore et al.). I propose that this sequence represents the track of the interaction region during the past 10 Myr or so. This hypothesis will perhaps be verified by refined hydrodynamical modeling in the near future.

4 Concluding Remark

It is evident from the results presented here that morphology remains a vital discipline in astronomical research.

Acknowledgments

I thank the SEA IX organizers for this kind invitation as well as generous travel and subsistence support. Ancillary support was provided by NASA through grant GO-10898.01 from STScI, which is operated by AURA, Inc., under NASA contract NAS5-2655.

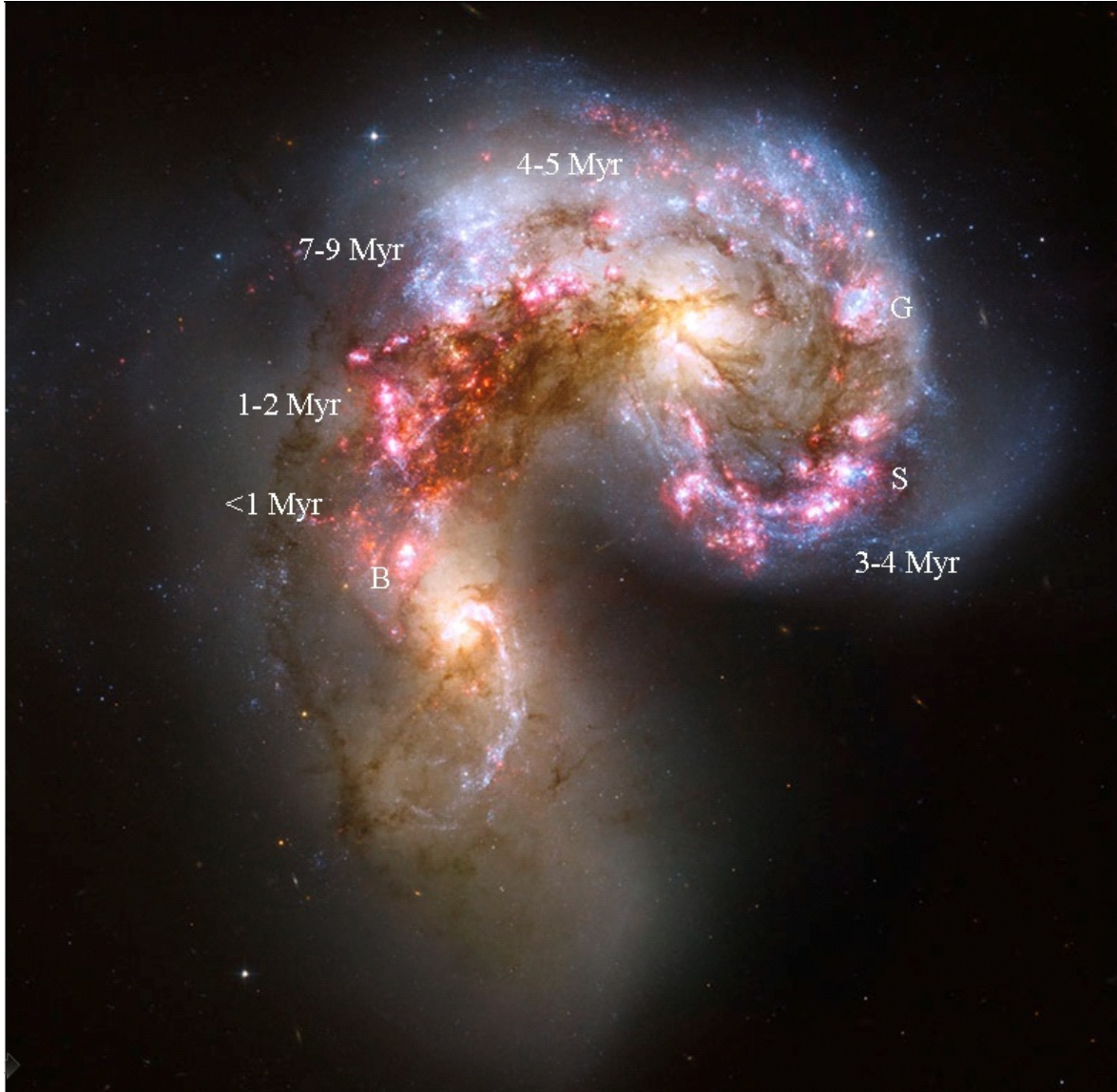


Figure 5: The Antennae major-merger starburst, as seen by the HST Advanced Camera for Surveys. The ages of various subregions are marked based on the morphologies of the multiple nebulae and clusters they contain; the most luminous Spitzer IR sources are located in the youngest. A monotonic, curving age sequence across the face of the system is revealed. The letters are designations of particular complexes by Whitmore et al. (2010).

References

- [1] Corti, M.A., Walborn, N.R., & Evans, C.J. 2009, *PASP*, 121, 9
- [2] Drissen, L., Roy, J.-R., Robert, C., Devost, D., & Doyon, R. 2000, *AJ*, 119, 688
- [3] Gray, R.O., & Corbally, C.J. 2009, *Stellar Spectral Classification* (Princeton University Press)
- [4] Howarth, I.D., & Smith, K.C. 2001, *MNRAS*, 327, 353
- [5] Karl, S.J., Naab, T., Johansson, P.H., Kotarba, H., Boily, C.M., Renaud, F., & Theis, C. 2010, *ApJ*, 715, L88
- [6] Klaas, U., Nielbock, M., Haas, M., Krause, O., & Schreiber, J. 2010, *A&A*, 518, L44
- [7] Langer, N., Cantiello, M., Yoon, S.-C., Hunter, I., Brott, I., Lennon, D., de Mink, S., & Verheijdt, M. 2008, in *IAU Symp. 250, Massive Stars as Cosmic Engines*, ed. F. Bresolin, P.A. Crowther, & J. Puls (Cambridge University Press), 167
- [8] Larsen, S.S., Efremov, Y.N., Elmegreen, B.G., Alfaro, E.J., Battinelli, P., Hodge, P.W., & Richtler, T. 2002, *ApJ*, 567, 896
- [9] MacKenty, J.W., Maíz-Apellániz, J., Pickens, C.E., Norman, C.A., & Walborn, N.R. 2000, *AJ*, 120, 3007
- [10] Maeder, A., & Meynet, G. 2000, *ARAA*, 38, 143
- [11] Martins, F., Donati, J.-F., Marcolino, W.L.F., Bouret, J.-C., Wade, G.A., Escolano, C., Howarth, I.D., & MiMeS 2010, *MNRAS*, 407, 1423
- [12] Sota, A., Maíz Apellániz, J., Walborn, N.R., Alfaro, E.J., Barbá, R.H., Morrell, N.I., Gamen, R.C., & Arias, J.I. 2011, *ApJS*, submitted
- [13] Teyssier, R., Chapon, D., & Bournaud, F. 2010, *ApJ*, 720, L149
- [14] Wade, G.A. et al. 2011, in preparation
- [15] Walborn, N.R. 2001, in *ASP Conf. Ser.*, 242, *Eta Carinae & Other Mysterious Stars*, ed. T. Gull, S. Johansson, & K. Davidson (San Francisco: ASP), 217
- [16] Walborn, N.R. 2002, in *ASP Conf. Ser.*, 267, *Hot Star Workshop III: The Earliest Phases of Massive Star Birth*, ed. P.A. Crowther (San Francisco: ASP), 111
- [17] Walborn, N.R. 2003, in *ASP Conf. Ser.*, 304, *CNO in the Universe*, ed. C. Charbonnel, D. Schaerer, & G. Meynet (San Francisco: ASP), 29
- [18] Walborn, N.R. 2010, in *ASP Conf. Ser.*, 425, *Hot and Cool: Bridging Gaps in Massive Star Evolution*, ed. C. Leitherer, P.D. Bennett, P.W. Morris, & J.Th. Van Loon (San Francisco: ASP), 45
- [19] Walborn, N.R., Barbá, R.H., Brandner, W., Rubio, M., Grebel, E.K., & Probst, R.G. 1999a, *AJ*, 117, 225
- [20] Walborn, N.R., Drissen, L., Parker, J.Wm., Saha, A., MacKenty, J.W., & White, R.L. 1999b, *AJ*, 118, 1684
- [21] Walborn, N.R., Maíz Apellániz, J., & Barbá, R.H. 2002, *AJ*, 124, 1601
- [22] Walborn, N.R., & Parker, J.Wm. 1992, *ApJ*, 399, L87

- [23] Walborn, N.R., Sota, A., Maíz Apellániz, J., Alfaro, E.J., Morrell, N.I., Barbá, R.H., Arias, J.I., & Gamen, R.C. 2010, *ApJ*, 711, L143
- [24] Walborn, N.R., Sota, A., Maíz Apellániz, J., Alfaro, E.J., Morrell, N.I., Barbá, R.H., Arias, J.I., & Gamen, R.C. 2011, in preparation
- [25] Wang, Z., Fazio, G.G., Ashby, M.L.N., Huang, J.-S., Pahre, M.A., Smith, H.A., Willner, S.P., Forrest, W.J., Pipher, J.L., & Surace, J.A. 2004, *ApJS*, 154, 193
- [26] Whitmore, B.C., Chandar, R., Schweizer, F., Rothberg, B., Leitherer, C., Rieke, M., Rieke, G., Blair, W.P., Mengel, S., & Alonso-Herrero, A. 2010, *AJ*, 140, 75
- [27] Zhang, H.-X., Gao, Y., & Kong, X. 2010, *MNRAS*, 401, 1839